Norwegian
Meteorological
Institute

METreport

No. 01/2019
ISSN 2387-4201
Oceanography

Analysis of co-located buoy measurements and wave model results

Birgitte R. Furevik, Ole Johan Aarnes, Anette Lauen Borg

Title Analysis of co-located buoy measurements and SWAN modeling	**Date** 18. January 2019
Section OM	**Report no.** No. 01/2019
Author(s) Birgitte Rugaard Furevik, Ole Johan Aarnes, Anette Lauen Borg	**Classification** ● Free ○ Restricted
Client(s) Aanderaa Xylem	**Client's reference** [Client's reference]

Abstract

This report is a deliverable of the MAROFF-DWS project "Fleksibel og kostnadseffektiv bølgesensor" (2016-2018), a Norwegian Research Council project under the MAROFF programme. The project had the aim of testing off-the-shelf accelerometers to develop low-cost wave sensor to be used onboard existing multi-purpose buoys.

This report describes the work on evaluation and use of the wave measurements performed west of Karmøy 2017-2018. The MOTUS wave sensor was put on two different large instrument buoys (Tideland and EMM2.0) placed together with a Directional Waverider in this offshore location. MOTUS performed very well against the Waverider on both buoys. The measurements was further used to verify two different wave model setups. In order to investigate the possibility for forecasting freak waves, freak wave recordings on the two buoys were matched against each other and against Benjamin-Feir index (BFI) from one model run. It was not possible to observe any relationship between sea state and freak wave occurrence, which makes it problematic to forecast these events.

As a result of the project, a Tideland buoy with MOTUS sensor , was deployed at Fauskane west of Ålesund in november 2018 by Kystverket. Wind, wave and current data from this buoy can be accessed at frost.met.no and thredds.met.no.

Keywords

wave buoy, freak waves, SWAN, wave modelling

Disciplinary signature

Responsible signature

Abstract

This report is a deliverable of the MAROFF-DWS project “Fleksibel og kostnadseffektiv bølgesensor” (2016-2018), a Norwegian Research Council project under the MAROFF programme. The project had the aim of testing off-the-shelf accelerometers to develop low-cost wave sensor to be used onboard existing multi-purpose buoys.

This report describes the work on evaluation and use of the wave measurements performed west of Karmøy 2017-2018. The MOTUS wave sensor was put on two different large instrument buoys (Tideland and EMM2.0) placed together with a Directional Waverider in this offshore location. MOTUS performed very well against the Waverider on both buoys. The measurements was further used to verify two different wave model setups. In order to investigate the possibility for forecasting freak waves, freak wave recordings on the two buoys were matched against each other and against Benjamin-Feir index (BFI) from one model run. It was not possible to observe any relationship between sea state and freak wave occurrence, which makes it problematic to forecast these events.

As a result of the project, a Tideland buoy with MOTUS sensor, was deployed at Fauskane west of Ålesund in november 2018 by Kystverket. Wind, wave and current data from this buoy can be accessed at frost.met.no and thredds.met.no.

Table of contents

1 Introduction

The MAROFF-DWS project "Fleksibel og kostnadseffektiv bølgesensor"[1] (2016-2018) was a Norwegian Research Council project led by Aanderaa Xylem which had the aim of testing off-the-shelf accelerometers to develop a low-cost wave sensor which may be used onboard different existing multi-purpose buoys. The task of MET was to give input to the development of parameters and evaluate the measurements. The present report is a summary of the activity.

1.1 Background

Wave measurements are useful in a wide range of applications within leisure and transport, and necessary for designing, accessing and operating different floating and bottom-fixed constructions. In coastal areas, wave conditions may change rapidly and makes it much more difficult than offshore to estimate the waves in one location based on measurements from another. In addition, coastal projects are often smaller with poorer economic returns or less demands on environmental measurements when compared to the petroleum activity offshore. This means that there is a need for a low-cost wave sensor which provide quality measurements.

Wave buoy measurements are rather costly as they are usually performed using a dedicated wave buoy, where the anchoring system is optimised for the buoy to record the waves freely. Using an existing instrument buoy as platform for a wave sensor, a thorough quality-check of resulting measurements need to be carried out. Buoy response testing numerically and in wave tank was performed by CMR and Aanderaa Xylem. A large part of the testing, filtering and tuning at sea was performed on a running basis by Aanderaa Xylem. These activities are reported elsewhere.

[1] Norwegian Research Council project number 256521

1.2 Project activities

The task of MET in the project "Evaluering av bølgesensor montert på bøye" was to validate wave model quality using the buoy measurements and possibly investigate the combined effect of waves and currents. Originally the idea was to inter-compare measurements from the buoys in a test period and then move them to a configuration useful for validation of coastal wave modelling. However, for practical reasons, the buoys were placed and remained all together at the Hywind location, 10 km west of the south-western tip of Karmøy until autumn 2018. The buoys and parameters are presented in Chapter 2. A wave model setup with a coastal resolution of 50 m was also planned, but since the area of interest was more offshore the resolution was increased to 250 m. The wave modelling activity is presented in Chapter 3. As an alternative to the planned coastal wave analysis, analysis of freak waves on the co-located buoys was carried out and is presented in Chapter 4. Finally, a MOTUS buoy was purchased by the Norwegian Coastal Administration during the project period, and a description of the parameters and data handling is included in Chapter 5. A short summary is found in Chapter 6.

2 Buoy measurements

Three buoys were deployed at the so-called Hywind-location 10 km off the southwestern tip of Karmøy in 2017.

2.1 Buoys

MOTUS wave sensor is integrated into the Tideland SB 138P MOTUS Buoy and YSI EMM 2.0 MOTUS Buoy[2]. In the project the two buoys were deployed by Aanderaa Xylem together with a traditional Waverider buoy from Datawell deployed by CMR. The co-location allowed for testing and comparison of the wave sensors and investigating the influence of e.g. currents on the buoy performance. Output to netCDF CF was developed and is described in Chapter 5. The buoys were located 10 km west of Karmøy at 59.149 N, 5.02 E.

2.2 Sensors

Both Tideland and EMM2.0 were equipped with a MOTUS wave sensor, a Doppler Current Sensor (DCP, Snr 25 on EMM2.0 and Snr 22 on Tideland) and a Gill weather station with wind anemometer. The EMM2.0 had in addition a Doppler Current Profiler (DCPS) and an extra MOTUS sensor put on the side of the buoy (off-center), in order to see if it would be possible to correct for this in the processing of the wave data. In the output files the wave sensors are given different numbers as shown in the table below.

Wave sensor	Description	Time period
#2	Center of EMM2.0	7 February 2017 - 30 April 2018
#4	Tideland	7 February 2017 - 24 August 2017
#7	Off-center of EMM2.0	7 February 2017 - 26 October 2017
#17	EMM 2.0 (replacing #17)	21 November 2017 - 30 April 2018

[2] https://www.aanderaa.com/media/pdfs/motus-wave-buoys-flyer.pdf

#18	Tideland (replacing sensor #4)	24 August 2017 - 30 April 2018
#1 / WR	Waverider	14 February 2017 - 30 April 2018

Change in wave integration time from 15 minutes to 30 minutes on 18 December 2017 makes it difficult to compare time series before and after this date. In addition, sensor #2 had a cable fault meaning that the software could not be updated together with the rest, and the time series show transients in the beginning and end of each record series.

From January 2018, the configuration of the sensors #17 and #18 are the same and is free of changes.

The Wave Mean Direction is defined from the energy spectrum in different ways on MOTUS and Waverider. It is calculated by Aanderaa Xylem from Waverider data using the recommended equations

$$X_{mean} = \sum_f E(f) \cdot \cos(D(f))$$

$$Y_{mean} = \sum_f E(f) \cdot \sin(D(f))$$

$$\theta_{mean} = atan2(Y_{mean}, X_{mean})$$

while on MOTUS,

$$X_{mean} = \sum_f \sqrt{E(f)} \cdot \cos(D(f))$$

$$Y_{mean} = \sum_f \sqrt{E(f)} \cdot \sin(D(f))$$

$$\theta_{mean} = atan2(Y_{mean}, X_{mean})$$

is used. This was implemented, since significant wave height is defined using $\sqrt{E(f)}$.

In spectral wave models, the mean wave direction is calculated from the full directional - frequency spectrum[3],

$$\mathrm{DIR} = \frac{180}{\pi} \arctan\left[\frac{\int \sin\theta E(\sigma,\theta) d\sigma d\theta}{\int \cos\theta E(\sigma,\theta) d\sigma d\theta}\right]$$

which we assumed is similar to the definition used in Waverider. We therefore recommend to use the same method as for Waverider for calculation for MOTUS in the future. In the project however, the first method was used and was not changed during the project period.

[3] https://www.ecmwf.int/sites/default/files/elibrary/2017/17739-part-vii-ecmwf-wave-model.pdf

3 Wave modeling

This section describes the three wave model runs performed in the project and validation against buoy observations.

3.1 SWAN wave model

SWAN is a 3rd generation spectral wave model designed for coastal areas and shallow water. The model simulate development of the two-dimensional (frequency-direction) wave spectrum in time and space, which is mainly due to advection of wave energy and the wind input, dissipation (wave breaking) and non-linear wave-wave interaction.

In this study, the model is setup with 36 directions (10° directional resolution) and 31 frequencies (0.0464 - 1.0 Hz) for the spectral resolution. The model uses a time step of 10 minutes, and output are archived every hour. Standard wave parameters are calculated from the 2D-wave spectrum.

A regular grid with spatial resolution of 250m and 336x489 grid cells (Figure 1) is used for two simulations with different wind input and boundary spectra denoted SWAN-NORA10 and SWAN-WAM4/MEPS.

SWAN was also tested on an unstructured grid covering approximately the same area, with coarse mesh offshore and 50m for finest grid cells close to shore (Figure 2).

Boundary spectra and wind input for SWAN-NORA10 was taken from the Norwegian hindcast of wind and waves (NORA10), developed at MET (Reistad et al., 2011). NORA10 has a horizontal resolution of 10-11km in both wind and waves. The archive is based on the atmosphere model HIRLAM (High-resolution limited area model) and the wave model WAM. This model setup was run for 1 January 2017 - 1 January 2018.

Boundary spectra and wind input for SWAN-WAM4/MEPS are taken from the operational forecast models, i.e. the wave model WAM with 4 km resolution and atmosphere model AROME with 2.5 km resolution. This model setup was run for 1 january 2017 - 31 January 2018.

Available output parameters from both model setups are listed in table 1. Spectra are only stored at the three buoy located very close together at Hywind.

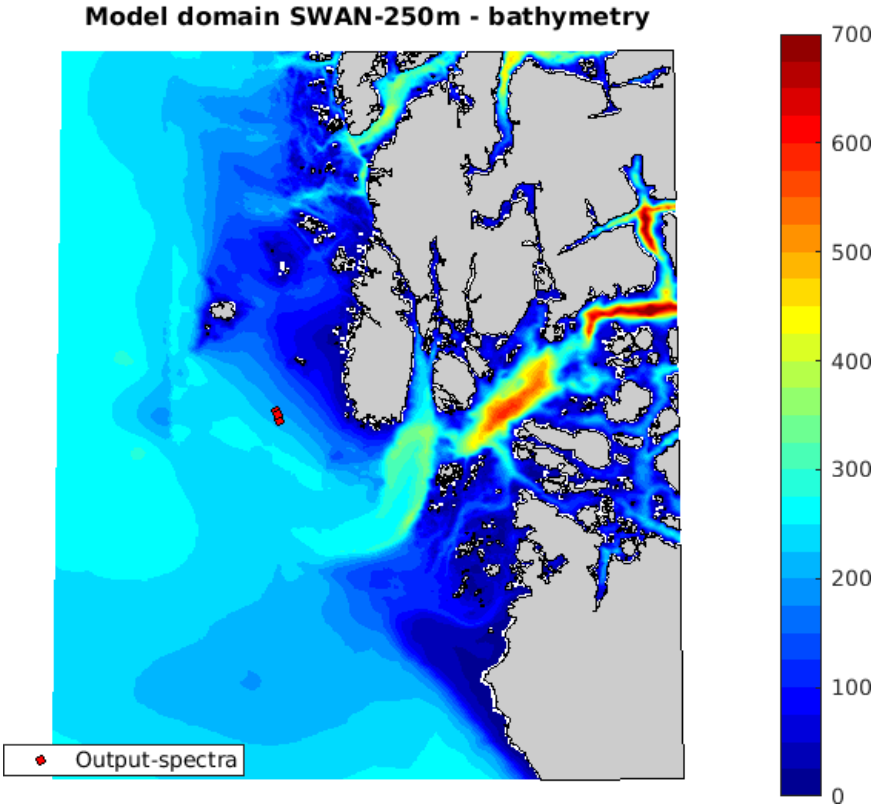

Figure 1: Bathymetry (depths in m) with Hywind position indicated in red, where the buoys are located. Output spectra (2D) are taken from the model in the three buoy locations.

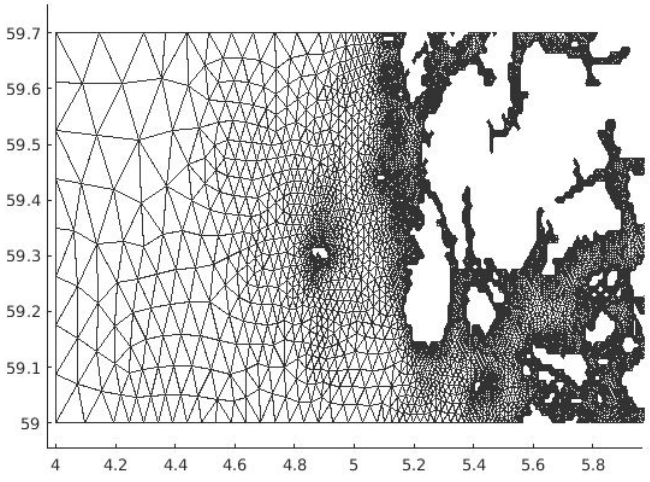

Figure 2: The unstructured grid which was tested in SWAN.

Table 1: Model systems and output.

Model system	Output parameters	Spectra locations
SWAN-NORA10	Significant wave height (Hs) Peak period (Tp) Peak direction (Pdir) Mean period (Tm01/Tm02) Mean direction (Mdir) Swell height (Hs-swell) Directional spread (Dspr)	
SWAN-WAM4/MEPS	Significant wave height (Hs) Peak period (Tp) Peak direction (Pdir) Mean period (Tm01/Tm02) Mean direction (Mdir) Swell height (Hs-swell) Directional spread (Dspr) Benjamin-Feir index (BFI)	

3.1.1 Regular grid (SWAN-NORA10 and SWAN-WAM4/MEPS)

A comparison of wind speed input (FF) and significant wave height putput (Hs) during 2017 between SWAN-NORA10 and SWAN-WAM4/MEPS show overall agreement for Hs 0-9m with some scatter (Figure 3). The few points during the highest wave situations (> 9m) are modeled 10% higher with the SWAN-WAM4/MEPS model system. This may be related to the slightly higher wind speed in MEPS as shown in Figure 3 (left). It should be noted that all points above 9m may be due to the same storm. The wave direction distribution in Figure 4 show that SWAN-WAM4/MEPS gives more westerly waves than SWAN-NORA10.

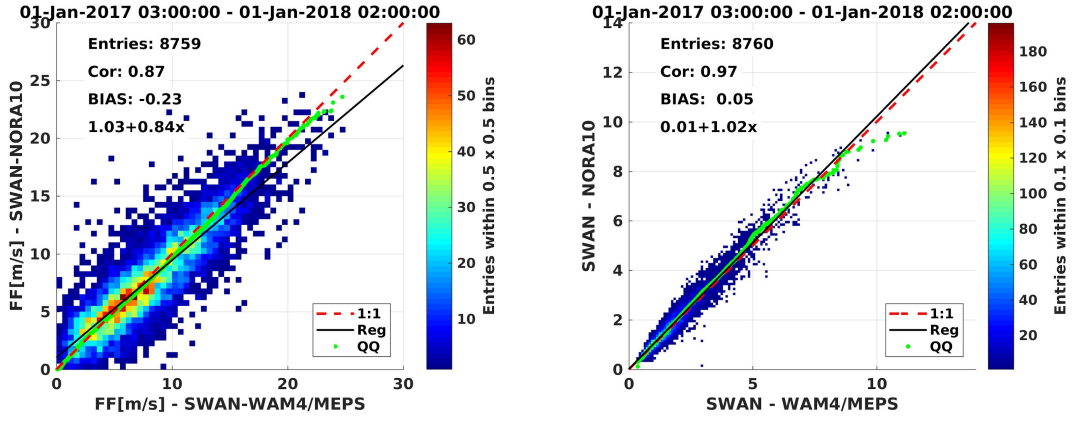

Figure 3: Comparison of wind speed (left) and significant wave height (right) during 2017 from two SWAN model setup; SWAN-NORA10 and SWAN-WAM4/MEPS.

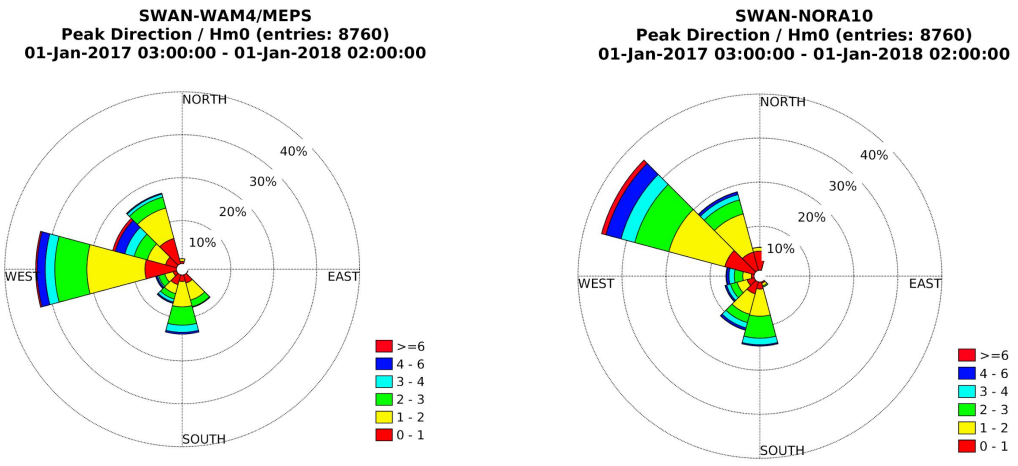

Figure 4: Wave rose showing peak wave direction from SWAN-WAM4/MEPS (left) and SWAN-NORA10 (right) for one year simulation.

3.1.2 Unstructured grid

Different mesh generators were investigated to create an unstructured grid suitable for stable runs with SWAN. In the end, mesh2D (Matlab) was the preferred routine.The mesh was generated so that cells with highest detail (50m) are found near the coastlines and coarse cells offshore. The grid does not automatically interpret the coast as a solid boundary, and open ocean grid cells to receive boundary spectra, needs to be defined. As the coastline in Norway is not necessarily associated with shallow water and offshore areas may be occasionally shallow, the grid should ideally be refined according to the water depth. An attempt was made to refine the grid in shallow areas. However, this created too many triangles related to some nodes. More than 7 is not accepted in SWAN.

SWAN was tested on the grid in stationary mode and with realistic boundary wave spectra and wind. An example of output from a stationary run with homogeneous easterly 20m/s winds is shown as a surface plot in Figure 5.

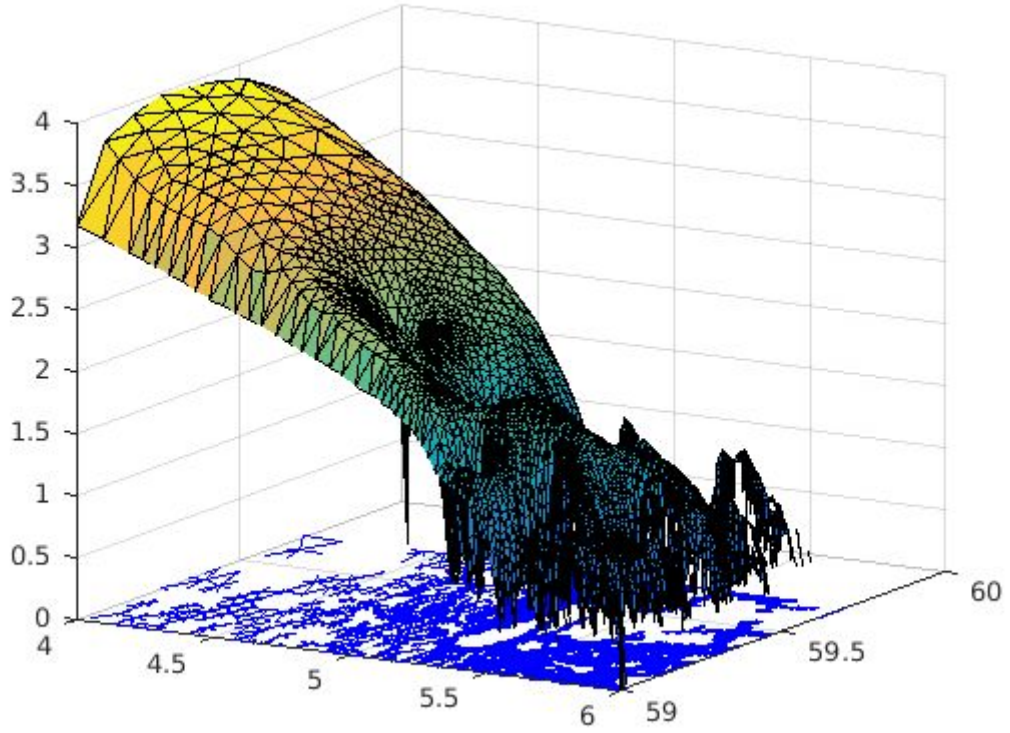

Figure 5: Surface plot of output Hs from SWAN stationary unstructured run with 20m/s easterly winds.

A practical challenge of using SWAN on unstructured grid at MET, is that it is not parallelized. It can run on more than one CPU, only if coupled with a different model code, such as ADCIRC (storm surge model from University of North Carolina) which is parallelized. However, it was decided during the project not to implement the ADCIRC, as this would require an effort beyond the strategy of MET-Norway, which is to limit, rather than expand, the model suite.

3.2 Model verification

Significant wave height from the two model setup are compared to measurements from the Waverider buoy (Figure 6). The comparison shows a slightly higher correlation 0.96 and less scatter with SWAN-WAM4/MEPS, but a better distributional behaviour by SWAN-NORA10. The higher waves from the SWAN-WAM4/MEPS system may be related to MEPS giving too high winds from 7 m/s and up compared to the Gill sensor onboard the Tideland buoy (Figure 7). The winds from the model is given at 10 m height above sea level and the buoy measures the wind in 4 m. Reducing 10 m/s wind in 10 m to 4 m using the power law (with alpha 0.06) gives 9.5 m/s which will account for some of the difference.

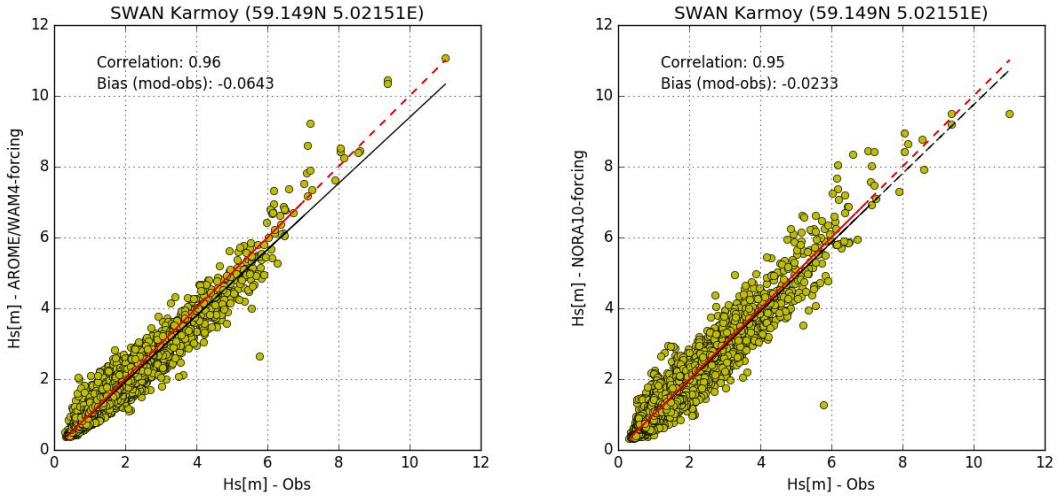

Figure 6: Scatterplots of Hs from SWAN-WAM4/MEPS (left) and SWAN-NORA10 (right) against waverider.

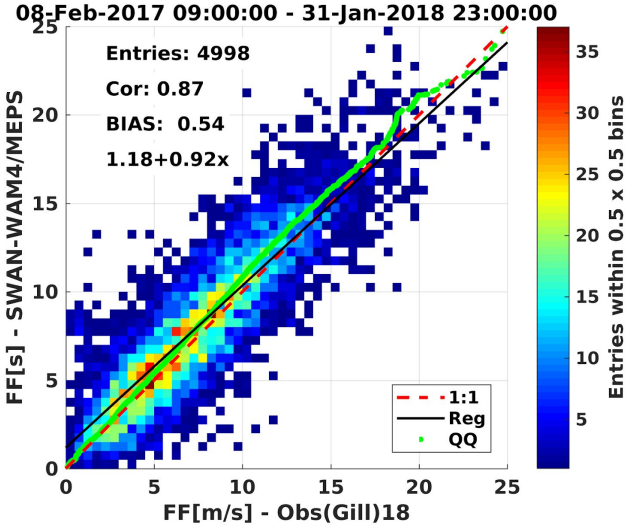

Figure 7: Comparison of MEPS wind speed against Gill wind sensor on Tideland buoy.

Scatter plots of Hs and Tp from SWAN-WAM4/MEPS against all six wave sensors at Hywind, is shown in Figure 8 and 9, respectively. SWAN-WAM4/MEPS compare quite similar to all of the sensors, even if the measurement periods are of different lengths. The highest Tp-values (20-25 s) from the buoys are most likely due to recordings while buoy is still on land (erroneous values).

Peak wave directions from three sensors are shown in Figure 10. The time periods are slightly different, so the wave roses at corresponding times from SWAN-WAM4/MEPS are plotted in the first row. It is clear that SWAN-WAM4/MEPS gives more waves from straight west than what is observed and that SWAN-NORA10 has a better distribution of the peak direction (see Figure 4).

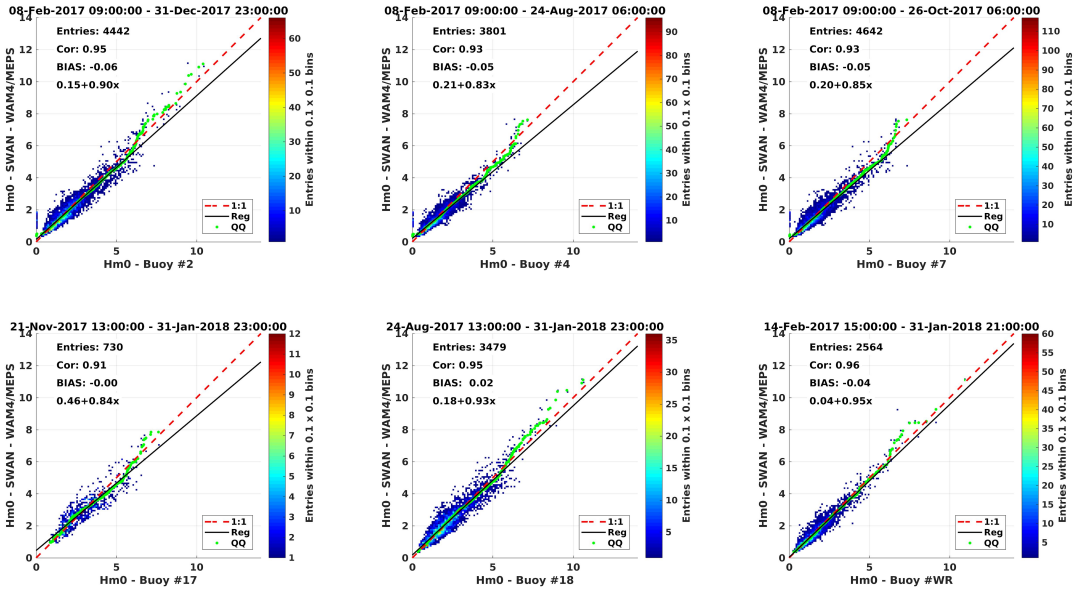

Figure 8: Comparison of Hs from SWAN-WAM4/MEPS with sensors 2, 4, 7, 17, 18 and waverider (WR).

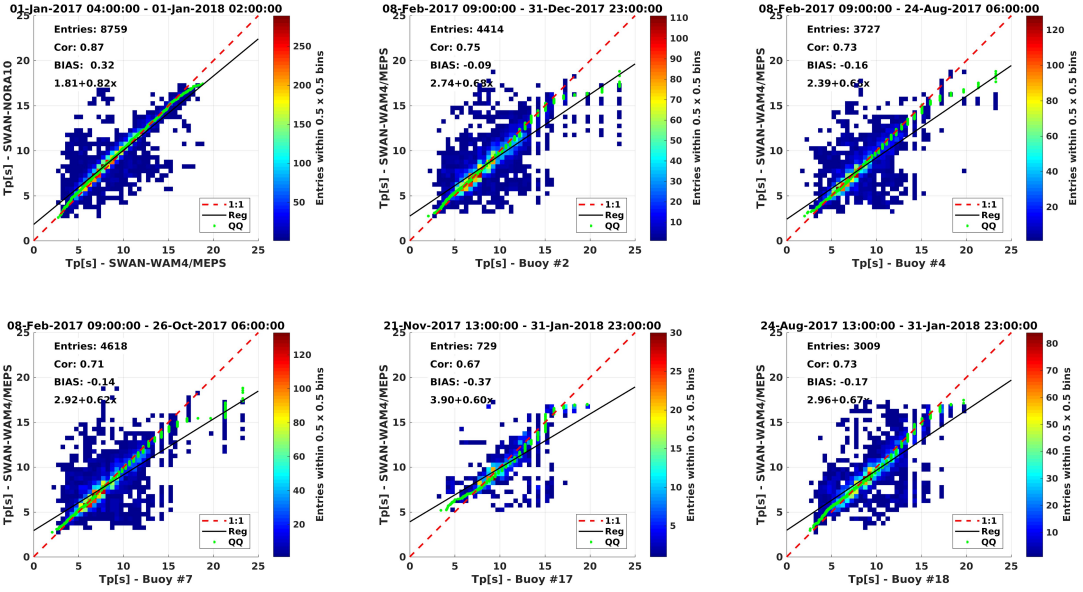

Figure 9: Comparison of Tp from SWAN-WAM4/MEPS with sensors 2, 4, 7, 17, 18 and waverider (WR).

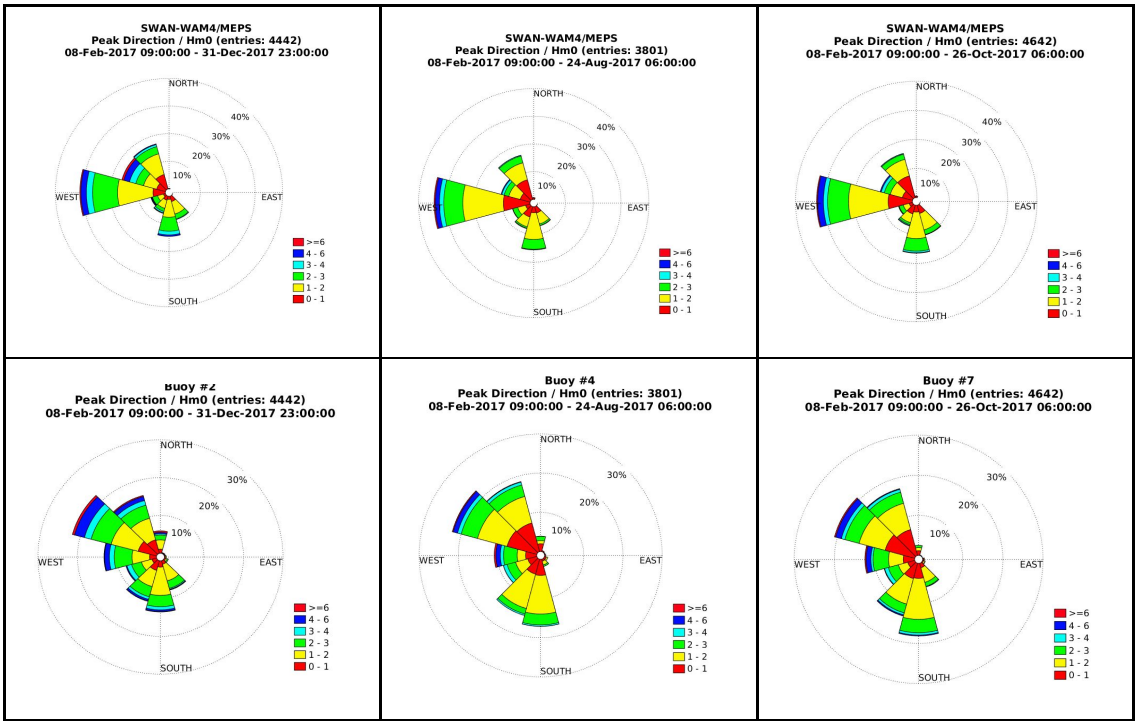

Figure 10: Wave roses from observations (lower row) and wave roses from the corresponding time periods from SWAN-WAM4/MEPS (upper row). The columns are for wave sensor 2, 4 and 7 from left to right. Please note that the time periods are different for each sensor.

3.3 Summary

Main results from the model verification are:

- Significant wave height and period corresponds well to observations.
- The longest buoy peak periods (20-25 s) are probably due to erroneous land recordings.
- Peak direction based on SWAN with forcing from the operational models (SWAN-WAM4/MEPS) is more westerly than SWAN with NORA10-forcing (SWAN_NORA10). SWAN-NORA10 corresponds on the other hand well to observations.

4 Freak wave analysis from co-located measurements

The EMM2.0 and Tideland buoys located close together allow for an investigation of the predictability of freak waves

4.1 Introduction

Freak or rogue waves are commonly defined as unusually large-amplitude waves that appear from nowhere in the open ocean. Perhaps the most famous freak wave, since it was the first ever recorded, is the new year wave at Draupner platform in 1995 (See e.g. Walker et al., 2004). Another recorded freak wave in the North Sea is the Andrea wave in 2007 at the Ekofisk oil field (Donelan and Magnusson, 2017). In 2016 the floating rig COSL Innovator at the Troll oil field was hit by a freak wave[4].

The Benjamin-Feir index (BFI) is the ratio between the wave steepness (Hs/L) and the wave bandwidth. Steep waves in a narrow frequency spectrum will give high BFI values. The statistical properties of a sea state with high BFI are supposed to be different, and favour the occurrence of freak waves (Janssen, 2003). The index goes between 0 and 1, with the median around 0.4. Wave models from the operational centres now output the BFI as a parameter, because it is desired to have an index that could be used to forecast when there is an increased risk of freak waves during storms. However, it has proven difficult to validate the BFI.

From time series of sea surface elevation, freak waves are defined as when the ratio between maximum wave height (trough to crest) to the corresponding significant wave height is larger than 2.2 (Hmax/Hs > 2.2) or if the maximum crest (mean sea level in the time series to top of crest) to significant wave height is larger than 1.25 (Cmax/Hs > 1.25). Gramstad et al. (2018) analysed one year of measurements from Ekofisk in the North Sea and found a tendency for slightly higher BFI in sea states where freak waves are recorded. In a frequency diagram of Hs/Tp, the freak waves also occur more often for steeper waves, from their data.

[4] https://sysla.no/offshore/53-aring-dode-momentant-da-kjempebolge-traff-rigg/

Since we have data from several buoys within a relatively small area (less than 1 km apart), we can investigate the simultaneous occurrence of freak waves at the buoys. If freak waves are more likely to occur in some sea states, we would expect that freak waves occur more or less at the same time on two buoys in the same area. Further we investigate the relationship between measured freak waves and the general sea state, and compare to the relationship between BFI and the general sea state. If BFI is a useful measure for freak waves at this location, a higher number of freak waves should be observed for the sea state with typically high BFI.

4.2 Freak waves from observations

We have used the parameters Hs, Hmax, Cmax and Tp from sensor 17 and 18 in the csv- and matlab-files through the matlab-software DataViewerBuoy provided by Aanderaa Xylem. Hs and Hmax from the two sensors in Figure 11 show a good agreement in Hs, but we see that there are discrepancies of Hmax and that larger differences occur in higher sea states, as expected.

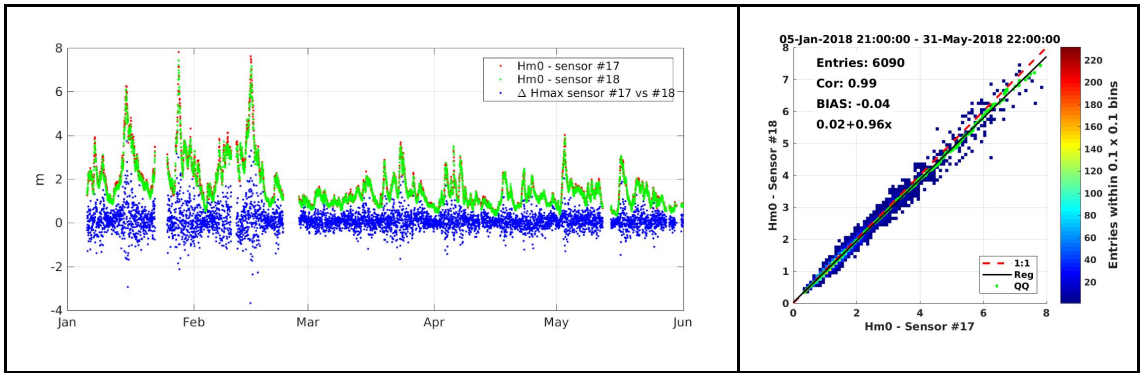

Figure 11: Time series January-May 2018 of Hs and the difference of Hmax (blue) from sensor 17 and 18 (left). Scatterplot of Hs from sensor 18 against 17 (right).

In Figure 12 we compare the same (17-minute) time periods on the two buoys, and plot Hmax/Hs and Cmax/Hs against each other. The green points represent the empirical QQ-plot, and shows the observations sorted in increasing order and plotted against each other. When they appear on a straight line as here, it shows that the distribution of the two data sets is very similar. This is not surprising since they come from the same type of wave sensor. It is however noticed that a freak wave is never observed at the same time on the two buoys.

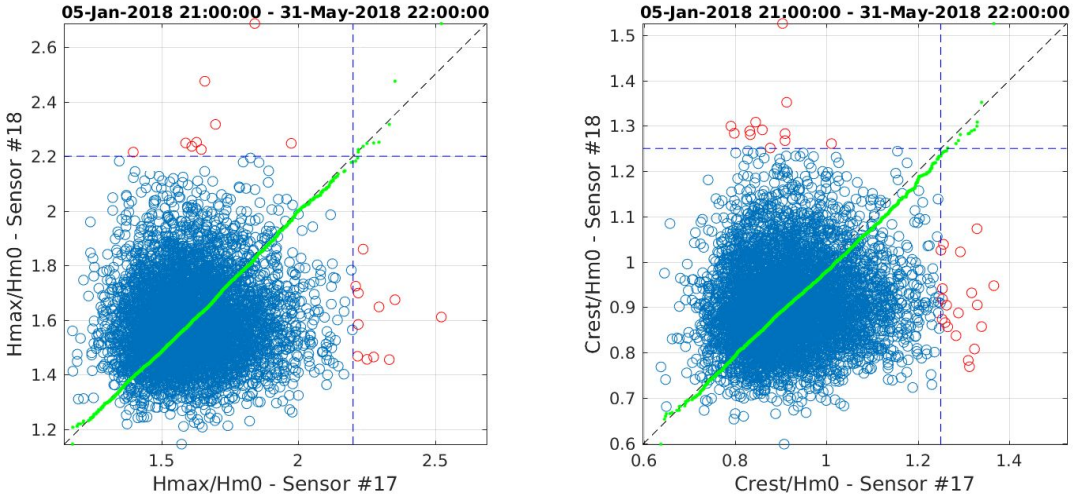

Figure 12: Simultaneous cases of Hmax/Hs (left) and Cmax/Hs (right) at the two sensors. Red points are recorded freak waves on one of the buoys. Green points is the empirical QQ-plot.

If a certain sea state is more likely to produce freak waves than another, freak waves may occur within a certain time frame at both buoys. Figure 13, however, shows that this is not the case for our dataset. Here we plot the maximum Hmax/Hs ratio from the two buoys within 4-hour intervals and still no red circles are recorded in the upper right corner.

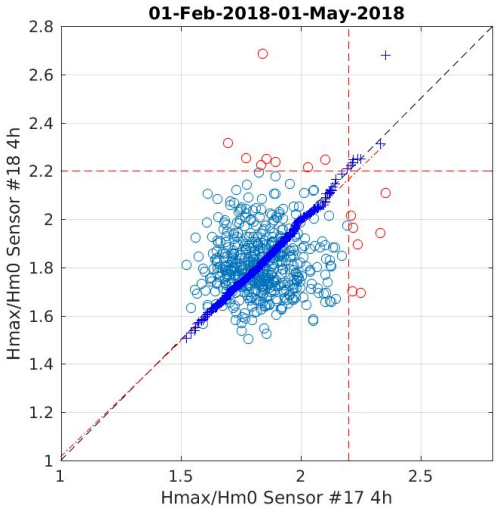

Figure 13: Maximum of ratio Hmax/Hs within 4-hours intervals at the two sensors. Red points are recorded freak waves on one of the buoys. Blue crosses is an empirical QQ-plot.

Crossing wind sea and swell, or local or remote currents may influence wave conditions and the likelihood of freak waves. From the data there seem to be no relation between the recorded freak waves and the current speed (not shown). Figure 14 shows the wind and current roses (top and bottom left). Winds are mainly from southeast and east while currents are going northwards. To the right occurence of freak waves in relation to wind and current direction are plotted. The colour scale gives the Hmax/Hs value and the length the percentage of recordings. Freak waves are recorded for all wind directions (figure 14 upper right), but mostly when the

wind is coming from the southeast quarter. With respect to currents, freak waves (lower right) appear in both northerly and southerly going currents, and even if northbound currents are clearly most frequent, half of the freak waves appear in southbound currents.

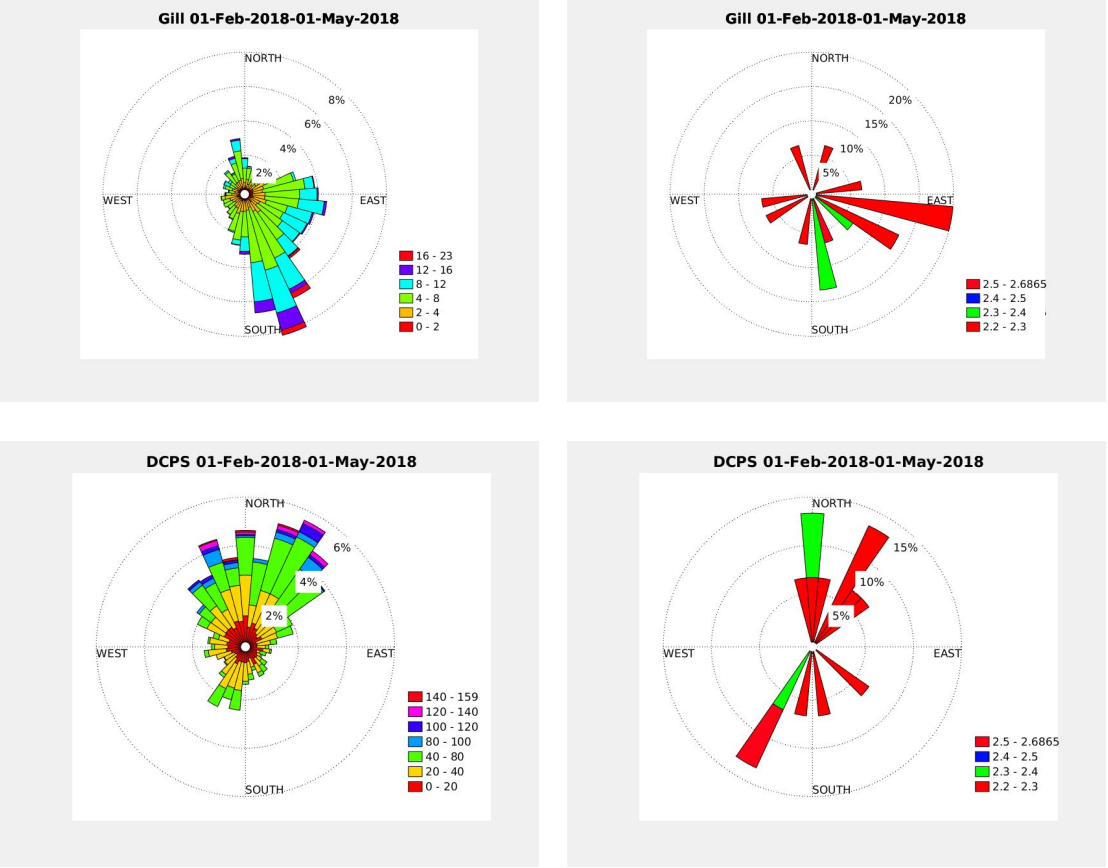

Figure 14: Windrose (top left) [m/s] and Current rose (bottom left) [cm/s]. Freak waves (Hmax/Hs>2.2 on any of #17 and #18) distributed on wind direction (top right) and current direction (lower right). Wind is plotted as "coming from" and current as "going to".

The total number of freak waves recorded on both buoys together is 15, which is too few for any real discussion. All the cases happened in sea states with Hs between 0.3 m and 2.2 m.

4.3 Freak waves and the BFI

Frequency tables from buoy and SWAN-WAM4/MEPS in Figure 15 show the occurrence of Hs and Tp combinations in percentage for the time period January-May 2018 (observations) and January-May 2017 (SWAN). Most frequent is sea states of 1-2 m Hs and peak periods of 5-10 s. There is an indication that EMM2.0 (#17) records steeper waves than Tideland. Keeping in mind that the time period is different, the steepness in SWAN seem to agree best with the Tideland buoy. The core of recordings in SWAN is 5-12 s Tp and 0-3 m Hs and has fewer recordings of low swell in the region 0-1 m Hs and 8-13 s Tp. These differences can partly be due to the different time periods, but may also indicate deficiencies in the model system. The frequency table for the full SWAN-WAM4/MEPS simulation period is shown in figure 16 for comparison.

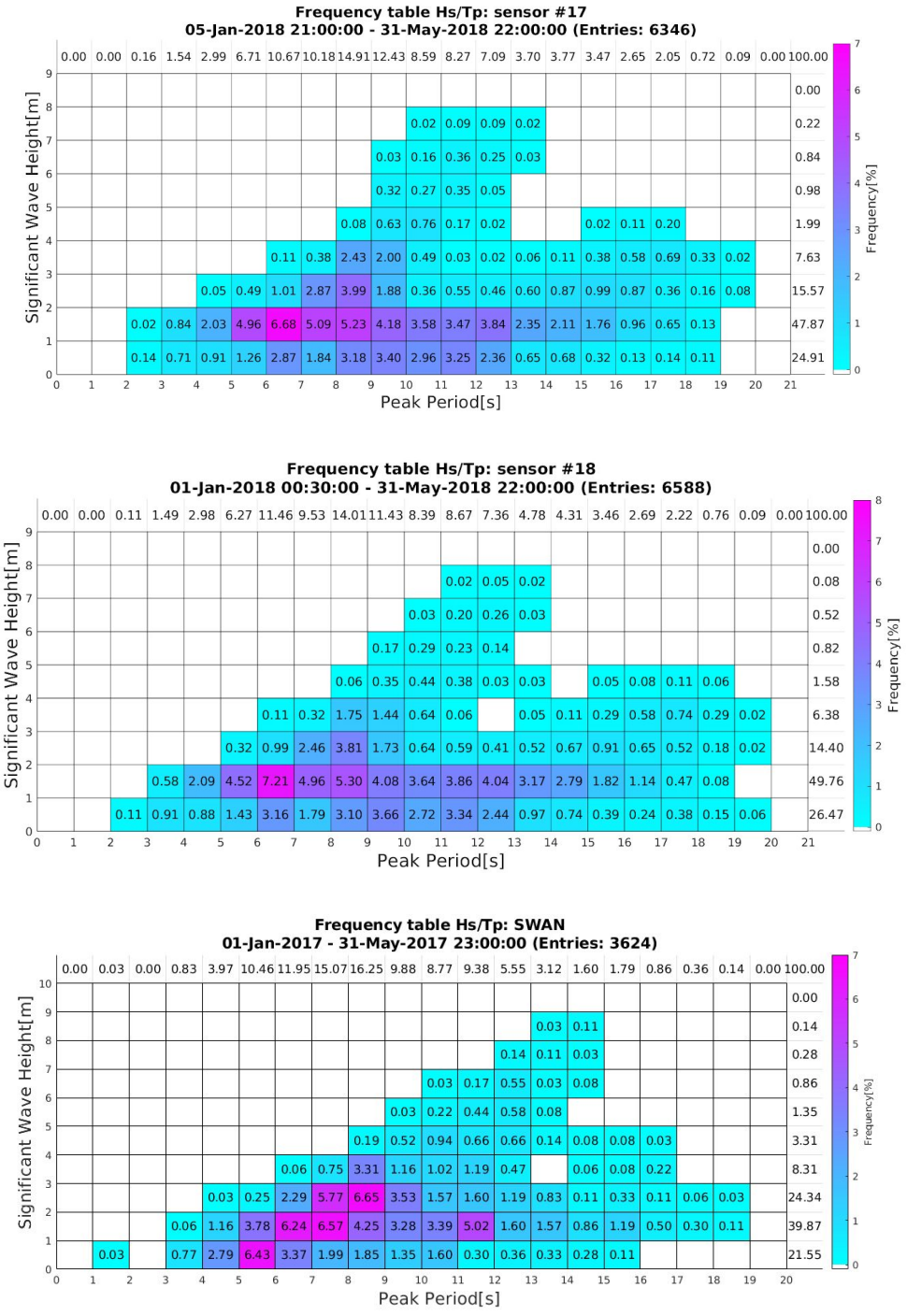

Figure 15: Frequency of occurrence of Hs and Tp from sensor 17 and 18 (top and middle). Frequency of occurrence of Hs and Tp from SWAN at buoy location from the same months the year before (2017) (bottom).

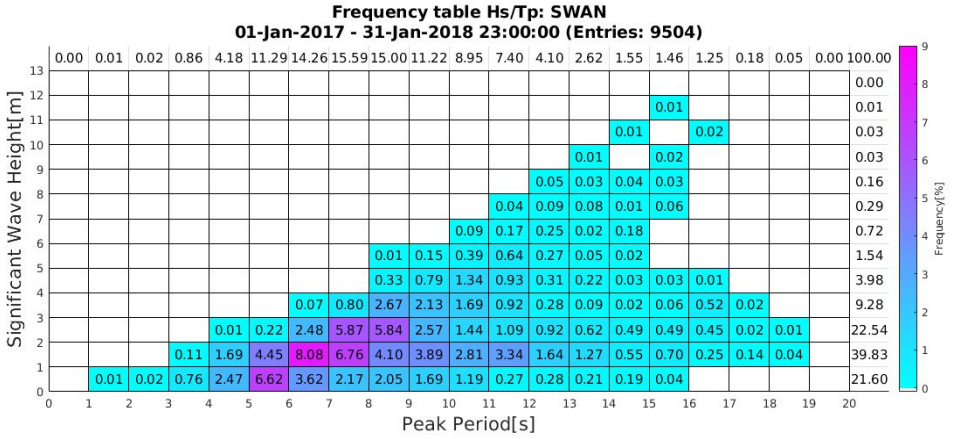

Figure 16: Frequency of occurrence of Hs and Tp from SWAN for 01-01-2017 to 31-01-2018 at the buoy location.

The BFI was produced as output from SWAN-WAM4/MEPS. A Hs-Tp plot of the mean and maximum BFI-values clearly relate the modelled freaky sea states (high BFI) to the steepest waves, which is also corresponding to growing wind sea (figure 17). However, the highest BFI-values are around 0.44, which is an average value for BFI calculated from the observations at Ekofisk (Gramstad et al. 2018). The 15 recorded cases with freak waves are observed in a general sea state, that can be found in the frequency tables. In figure 18, the freak wave incidences are marked on the frequency tables from the two buoys, in the Hs-Tp sea state that they appeared in. It is clearly seen that they are quite evenly distributed over the area with the most frequent sea states and not for example in the area with the steepest waves. This rather negative result is supported by Gramstad et al. 2018 with their analysis of Ekofisk data.

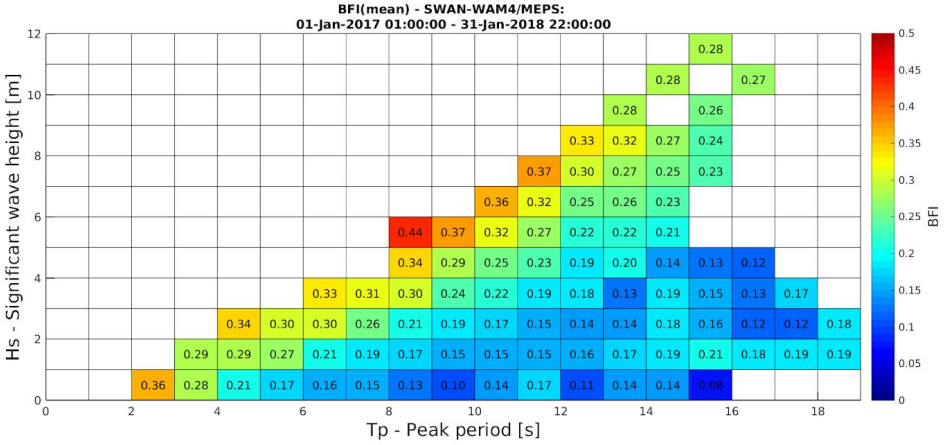

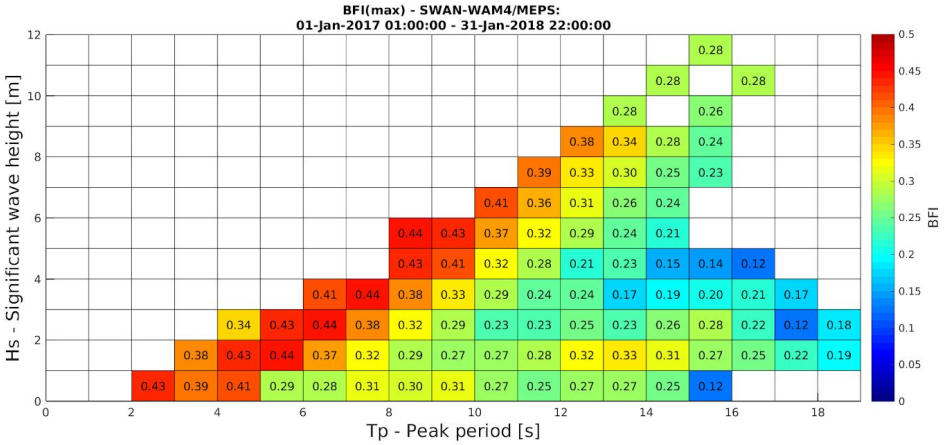

Figure 17: Mean and maximum BFI from SWAN-WAM4/MEPS model run for January-May 2018 at the buoy location.

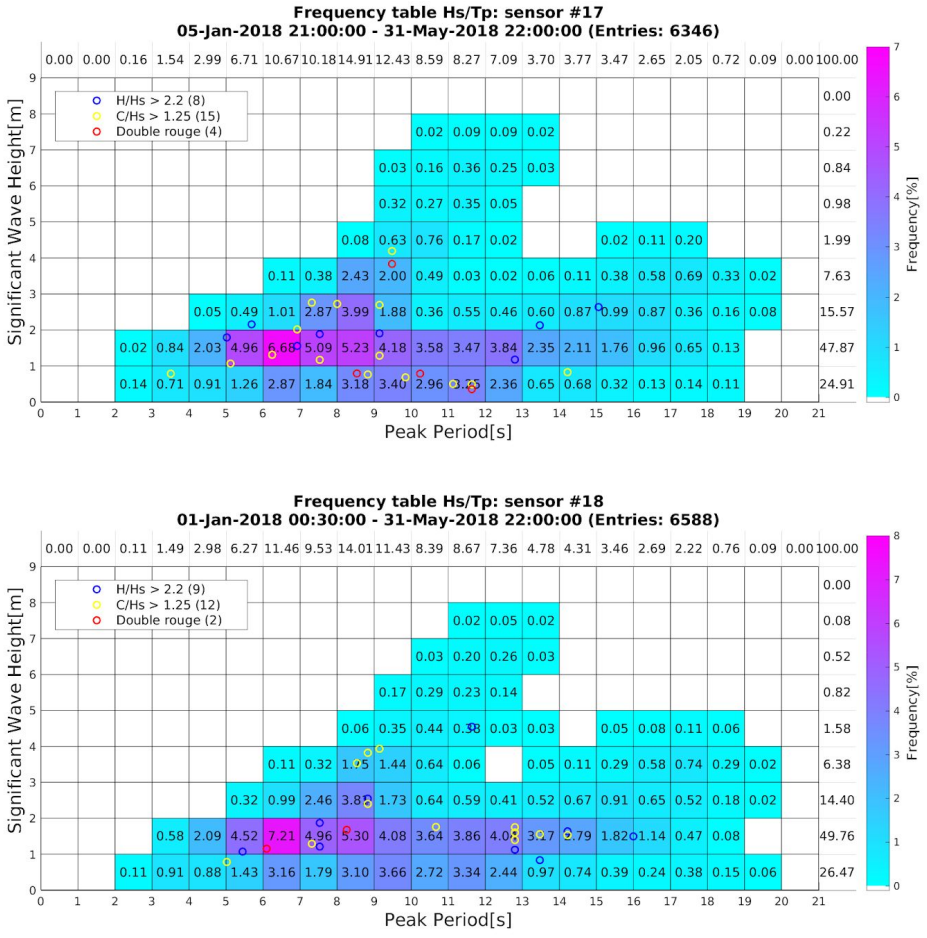

Figure 18: Same as Figure 15, but overlayed with circles are the recorded freak waves, colours refer to different criteria: Hmax/Hs > 2.2 (blue), Cmax/Hs > 1.25 (yellow) and when both criteria are fulfilled (red).

4.4 Discussion

The time period is rather short, and the total number of freak waves recorded on both buoys together is 15, which is too few for any statistical analysis. All the cases happened in sea states with Hs between 0.3 m and 2.2 m.

From our data, freak waves seem to occur in all sea states and are thus more likely to be observed in the sea states that are most common, simply since there are more wave observations. The Benjamin-Feir index (BFI) calculated from spectral wave model data, indicates that the highest risk of freak waves is for steep waves (growing wind sea), which thus does not agree with observations. Gramstad and Trulsen (2007) investigated the theoretical potential for BFI to be used in forecasting and conclude: "*For short crest lengths the statistics of freak waves deviates little from Gaussian and their occurrence is independent of group length (or Benjamin–Feir index, BFI). For long crest lengths the statistics of freak waves is strongly non-Gaussian and the group length (or BFI) is a good indicator of increased freak wave activity*". Long crests means here longer than 10 wavelengths. So there would be a forecasting potential in BFI if the crest length was known from the wave model. However, crest length is a difficult parameter to observe and forecast. Gramstad et al. (2018) found in the statistics slightly higher values of BFI for situations where freak waves were recorded than for other situations.

From our limited data set, we see no correlation between freak wave occurrence and current speed, while there may be a relation to current direction. The current is practically always northbound, while the current rose with freak waves show that half of the freak waves appear during southgoing currents (figure 14). Comparing wind direction and current direction for these cases show that some of them could be due to opposing currents, but the signal is not clear and this has not been investigated in detail.

5 Project spin-off: Real-time measurements from buoy at Fauskane, Møre og Romsdal

A fully operational buoy was purchased by Kystverket to replace a light buoy at Fauskane outside Ålesund. Real-time data are made available back to Kystverket and the public through the application programming interface (API) of MET.

5.1 First measurements from Fauskane

The buoy is located on the shelf west of Ålesund, just north of the entrance Breisundet to Sulafjord in 62.56 N 5.726 E (figure 19). The water depth is 40 m.

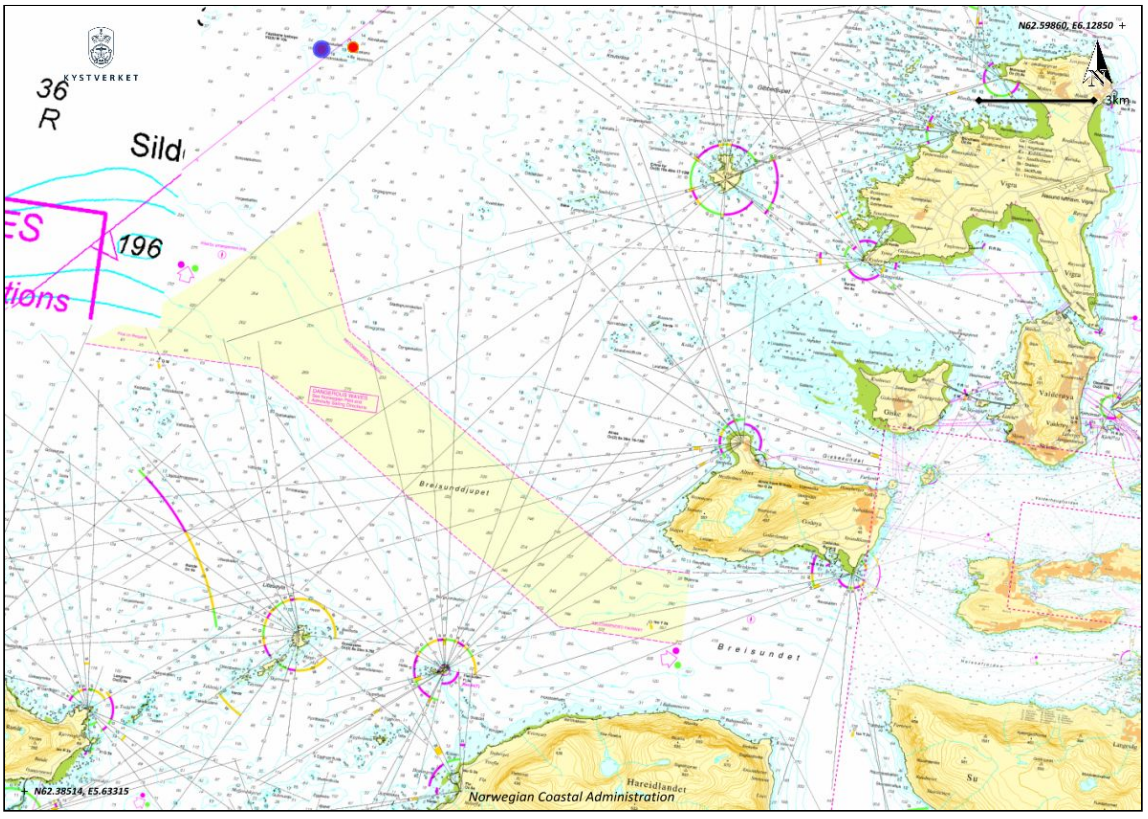

Figure 19: Part of sea chart showing the location of Fauskane light buoy (blue point).

The buoy is equipped with a Motus wave sensor, a Doppler Current Profiler and a Gill wind sensor and weather station. An example plot of Hs and current speed in 6m depth for December 2018 is shown in figure 20. An overview of the variables is presented in table 2.

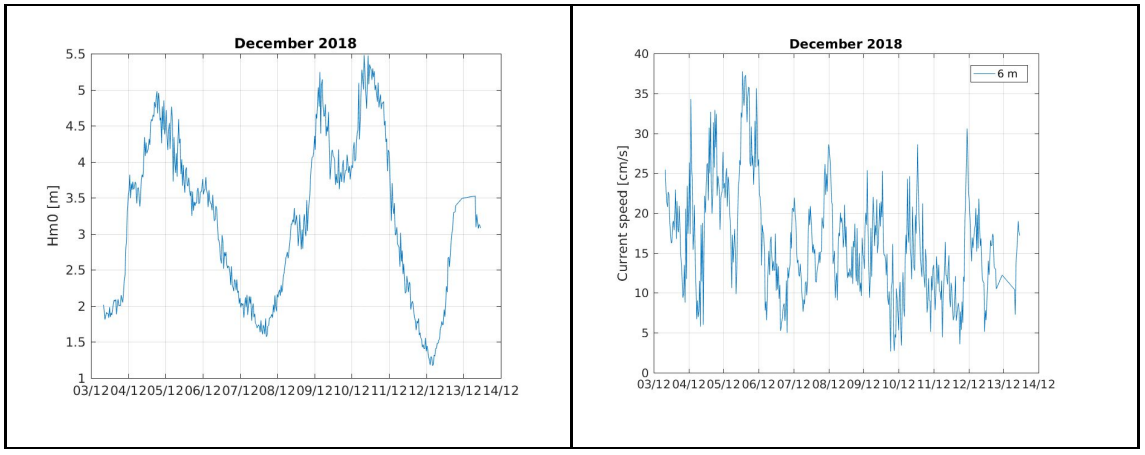

Figure 20: Sample significant wave height and current speed (6m depth) from Fauskane buoy.

Table 2: Name of the parameters in the netCDF-files produced by Aanderaa Xylem, the standard names used and the corresponding element in API (frost.met.no). The parameters without an element in the API are not included there.

Parameter in netCDF (thredds)	**Standard name set in the netCDF-files**	**Element in API (frost.met.no)**
Gust_Direction	wind_gust_from_direction	wind_from_direction_of_gust PT10M
Gust_Speed	wind_speed_of_gust	wind_speed_of_gust
Average_Wind_Direction	wind_from_direction	wind_from_direction
Average_Wind_Speed	wind_speed	wind_speed
Dewpoint	dew_point_temperature	
Temperature	air_temperature	air_temperature
Absolute_Humidity	specific_humidity	
Relative_Humidity	relative_humidity	relative_humidity
Pressure_at_Sea_Level	air_pressure_at_sea_level	air_pressure_at_sea_level
Long_Crestedness_Parameters*	sea_surface_wave_directional_spread	
First_Order_Spread *	sea_surface_wave_directional_spread	
Mean_Spreading_Angle*	sea_surface_wave_directional_spread	

Wave_Period_Tz	sea_surface_wave_mean_period	
Wave_Period_Tmax	sea_surface_wave_period_of_highest_wave	
Wave_Height_Trough	sea_surface_wave_maximum_trough_depth	
Wave_Height_Crest	sea_surface_wave_maximum_crest_height	
Wave_Height_Hmax	sea_surface_wave_maximum_height	max(sea_surface_wave_height PT10M)
Wave_Height_Wind_Hm0	sea_surface_wind_wave_significant_height	
Wave_Height_Swell_Hm0	sea_surface_swell_wave_significant_height	
Wave_Peak_Period_Wind	sea_surface_wind_wave_period_at_variance_spectral_density_maximum	
Wave_Peak_Period_Swell	sea_surface_primary_swell_wave_period_at_variance_spectral_density_maximum	
Wave_Peak_Period	sea_surface_wave_period_at_variance_spectral_density_maximum	sea_surface_wave_period_at_variance_spectral_density_maximum
Wave_Mean_Period_Tm02	sea_surface_wave_mean_period_from_variance_spectral_density_second_frequency_moment	
Wave_Peak_Direction_Wind	sea_surface_wind_wave_from_direction	
Wave_Mean_Direction	sea_surface_wave_from_direction	from_direction_of_mean(sea_surface_wave_total_energy PT10M)
Wave_Peak_Direction_Swell	sea_surface_primary_swell_wave_from_direction	
Wave_Peak_Direction	sea_surface_wave_from_direction_at_variance_spectral_density_maximum	
Significant_Wave_Height_Hm0	sea_surface_wave_significant_height	sea_surface_wave_significant_height_from_spectrum
Vertical_Speed	upward_sea_water_velocity	
Direction	sea_water_to_direction	sea_water_to_direction
Horizontal_Speed	sea_water_speed	sea_water_speed
latitude	latitude	latitude

longitude	longitude	longitude

* As defined in Kumar and Anoop (2013)

5.2 Solution for data transfer and user access

The buoy transfers the sensor measurements to a server owned by the buoy provider every 10 minutes (every 30 minutes during wintertime). The data format is converted from ascii to NetCDF and the resulting files are sent to a virtual server belonging to MET Norway via sftp as soon as they are ready.

MET Norway has systems already in place to perform quality control on buoy data and to track any delays in the data stream. These systems also publish data automatically through an API (Application Programming Interface) at https://frost.met.no. The API is open to the public and provides metadata as well as the quality controlled buoy measurements.

Data from the buoy are also published as open access monthly data sets through http://thredds.met.no. THREDDS (Thematic Real-time Environmental Distributed Data Services) is a web server that provides metadata and data access for scientific datasets, using a variety of remote data access protocols such as OPeNDAP (Open-source Project for a Network Data Access Protocol).

5.2.1 Access to data

Instructions on how to start downloading data from https://frost.met.no can be found here: https://frost.met.no/concepts#getting_started

The location of the monthly datasets on the THREDDS server is http://thredds.met.no/thredds/catalog/obs/kystverketbuoy/catalog.html
The datasets are available as NetCDF files; either downloaded manually or using programs such as curl or wget to collect the files automatically through OPeNDAP.

6 Summary

Verification of modeling results, investigation of freak wave occurrence and a new buoy in operation

The scope of the work package “Evaluering av bølgesensor montert på bøye” changed a few times during the project, partly as a consequence of the location of the buoys, and partly following the results from the activity.

A buoy is a excellent tool to verify a wave model. In particular having several buoys over an area where waves are changing due to sheltering, refraction, wave breaking or other reasons, provide a chance to verify the model and even look into reasons for any discrepancies that are seen. In this project, three buoys were deployed close together 10km from land in 200m water depth. EMM2.0 and Tideland with Motus wave sensors onboard were compared with a traditional Waverider. This intercomparison was an important part of the project, as it ensured the quality of the new flexible wave measurement device. However, this constellation of buoys is not ideal for investigation of wave models, as most models are doing reasonably fine offshore. When approaching coasts, difference in e.g. resolution may give larger differences. Thus, we have mainly used the buoys as verification for the wave models and looked at the effect of the different forcing (resolution held constant).

Around 15 freak waves were identified from the buoy data set. From the analysis it has not been possible to find relationships between occurrence of freak waves to the Benjamin-Feir index nor between the freak wave occurrence on the co-located buoys. It should be noted that the data set is probably too short to conclude.

Finally, we report on the data handling from the new Tideland buoy which was put into operation by Kystverket at Fauskane, west of Ålesund. Hopefully, this will be the first of many measuring light buoys on the coast.

An editorial introduction to the special issue based on the The 1st International Workshop on Waves, Storm Surges and Coastal Hazards incorporating the 15th international workshop on wave hindcasting and forecasting to appear in Ocean Dynamics was written with the support of this project (Swail et al., 2019).

Acknowledgements

The work was part of the Research Council of Norway MAROFF-programme project grant 256521.

References

Donelan, M. A. and Magnusson, A.-K. (2017) The Making of the Andrea Wave and other Rogues, *Sci. Rep*. 7, 44124; doi: 10.1038/srep44124.

Gramstad, Odin, Elzbieta Bitner-Gregersen, Øyvind Breivik, Anne Karin Magnusson, Magnar Reistad, Ole Johan Aarnes (2018) Analysis of rogue waves in North-Sea in-situ surface wave data, *Proceedings of the 37th International Conference on Ocean, Offshore and Arctic Engineering*, OMAE2018-77810, June 17-22, 2018, Madrid, Spain.

Gramstad, O. and K Trulsen (2007) Influence of crest and group length on the occurrence of freak waves, *Journal of Fluid Dynamics*, https://doi.org/10.1017/S0022112007006507

Janssen, Peter A. E. M. (2003) Nonlinear Four-Wave Interactions and Freak Waves, *Journal of Physical Oceanography*, https://doi.org/10.1175/1520-0485(2003)33%3C863:NFIAFW%3E2.0.CO;2

Kumar, V.S, and T.R. Anoop (2013) Directionality and spread of shallow water waves along the eastern Arabian Sea, *Annales Geophysicae*, 31, 1817–1827, 2013. DOI: https://doi.org/10.5194/angeo-31-1817-2013

Reistad, M., Ø. Breivik, H. Haakenstad, O. J. Aarnes, B. R. Furevik, and J.-R. Bidlot (2011), A high-resolution hindcast of wind and waves for the North Sea, the Norwegian Sea, and the Barents Sea, *J. Geophys. Res.*, 116, C05019, https://doi.org/10.1029/2010JC006402

Swail, V., J.H. Alves, Ø Breivik, J Brown, D Greenslade (2019) The 1st International Workshop on Waves, Storm Surges and Coastal Hazards incorporating the 15th international workshop on wave hindcasting and forecasting, editorial summary for special issue after the workshop, to appear in *Ocean Dynamics*.

Walker, D.A.G., P.H. Taylor and R. Eatock Taylor (2004) The shape of large surface waves on the open sea and the Draupner New Year wave, *Applied Ocean Research*, Volume 26, Issues 3–4, Pages 73-83. DOI: 10.1016/j.apor.2005.02.001